## CHAPTER 96

# Wave Climate of Large Reservoirs and a Revised Wave Hindcast Formula

Pierre Dupuis[1], Jean-Pierre Tournier[1], Octave Caron[2]


### Abstract

Since impounding of the various reservoirs of the La Grande Complex in northern Québec, the riprap of several dams and dykes has suffered some damage during the fifteen-year period that followed. A mandate was given to the Société d'énergie de la Baie James (SEBJ) in January 1992 to review the riprap design and evaluate the necessary repairs. This paper focuses on the revaluation of the design wave with revised wave hindcast formulas based on the large amount of wind and wave data collected.


### Introduction

Damage was observed to the riprap of some of the 215 embankment dams and dykes during the fifteen years since impoundment for the various reservoirs of the La Grande Hydroelectric Complex in northern Quebec. In January 1992, La Société d'énergie de la Baie James (SEBJ) was mandated by Hydro-Québec to review the riprap design and performance and to evaluate the necessary repairs. To fulfill its mandate, SEBJ conducted extensive field studies, including wind and wave measurements from four reservoirs and large scale model testing of repair schemes with irregular waves. Model testing is described by Mansard et al. (1996) while riprap repairs and design are presented by Tournier et al. (1996).

### Wind and Wave Data Acquisition

Extensive field measurements were made from 1992 to 1995 (SEBJ, 1996a) to establish the wave climate on four large reservoirs of the La Grande Complex that are located within the area delimited by 52 to 55°N of latitude and 67 to 79°W of longitude (figure 1). Wind speed and direction, wind gust and air temperature were monitored continuously and logged every five minutes at three nearby airports and six small islands on the reservoirs by Aanderaa weather stations.


[1] La Société d'Énergie de la Baie James, 500 Boul. René-Lévesque Ouest, Montréal, Québec, Canada, H2Z 1Z9

[2] Hydro-Québec, 800 Boul. De Maisonneuve Est, Montréal, Québec, Canada, H2L 4M8


**Figure 1.** La Grande Hydroelectric Complex

**Figure 2** WaveTrack buoy

WaveTrack buoys (0,9m diameter sphere) recorded wave trains for 17 minutes at the start of every hour at a sampling frequency of 2 Hz (figure 2). Raw data from the buoy accelerometer and tilt sensors were sent ashore via telemetry to a computer and archived for later processing. Over the four years, 9 different wave sites were monitored. In all, over 38 000 wave records were obtained for the ice free period that lasts from mid-June to the end of October.

This paper focuses on the dyke TA-13 mooring site, in the northern part of the LG-3 reservoir, for which over 9000 records cover all four years and where the most energetic episodes were recorded ($H_{mo}$ = 2,4 m in September, 1992). The buoy was moored a few kilometers south of the dyke in order to monitor various fetch length conditions. A weather station was erected nearby on a flat island to record the overwater wind. The wave acceleration record values are processed in the frequency domain to yield the significant wave height ($H_{mo}$) and the mean period ($T_{02}$), as defined in IAHR/PIANC (1986). They form the basic set of variables used in further analysis. This is acceptable since evaluation of wave height ratios (figure 3) indicate good agreement with the

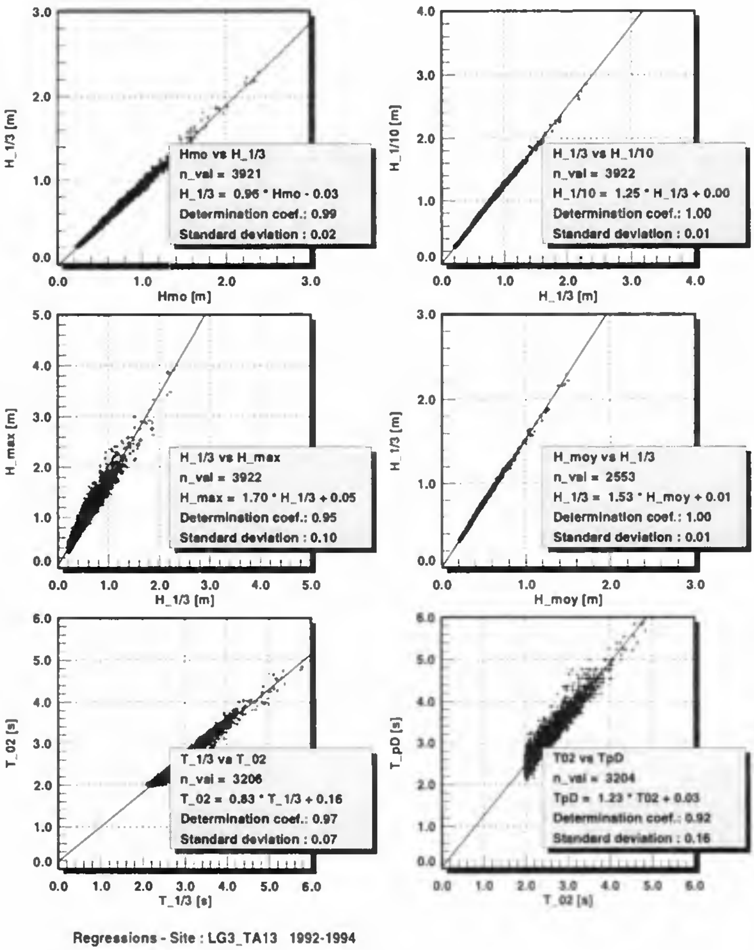


**Figure 3**. Wave parameter ratios for site TA-13.

Rayleigh distribution. These results are satisfactory for design purposes.

As shown on figure 4, similarity between wind speed and wave height response signals is evident, and similar results are obtained for all sites. This is indicative of the quick response of the body of water to the wind input. It can be noted that the wave steepness attains a limiting value in the vicinity of 0,06 for quite different wave conditions when $T_{02}$ is used. This indicates that the wave energy growth or decay, due to the wind is such that the ratio of wave height to wave length remains the same, when limiting conditions exists. This is very important since it will be used in determining the correct set of values for the various dimensional parameters.

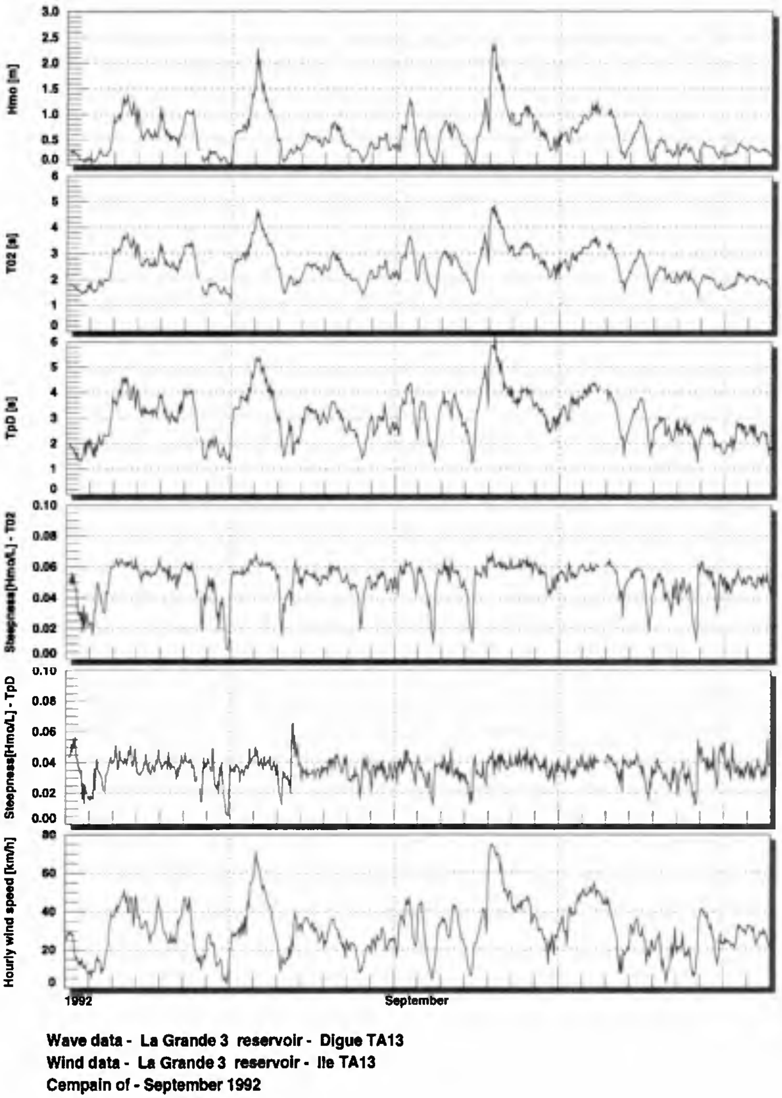


**Figure 4**. Typical measurements

## Dimensional analysis

Based on dimensional considerations, Bretschneider (1965) derives these relations:

$$\frac{gH}{U^2} = \psi_1\left[\frac{gF}{U^2}, \frac{gt}{U}\right] \qquad [1]$$

$$\frac{C}{U} = \psi_2\left[\frac{gF}{U^2},\ \frac{gt}{U}\right] \text{ or equivalently } \frac{gT}{U} = \psi_3\left[\frac{gF}{U^2},\ \frac{gt}{U}\right] \quad [2]$$

With $H$ the wave height, $T$ the period, $F$ the fetch length, $U$ the wind speed and $t$ the duration. $\psi_1$ and $\psi_2$ are functional relations that must be determined using wave data. Different editions of the Shore Protection Manual (CERC, 1977, 1984), noted SPM77 and SPM84, suggest the following:

| | | | |
|---|---|---|---|
| SPM 77 | $\frac{gH}{U^2} = 0{,}00354 \left(\frac{gF}{U^2}\right)^{0{,}42}$ | $\frac{gT}{U} = 0{,}581 \left(\frac{gF}{U^2}\right)^{0{,}25}$ | [3] |
| SPM 84 | $\frac{gH}{U_a^2} = 0{,}00160 \left(\frac{gF}{U_a^2}\right)^{0{,}50}$ | $\frac{gT}{U_a} = 0{,}286 \left(\frac{gF}{U_a^2}\right)^{0{,}333}$ | [4] |

where the hyperbolic functions found in the SPM84 are linearized in order to help to compare values from both editions and $U_a$ is the wind stress factor as defined in SPM84. Use of these formulas, however, results in poor hindcast, with over prediction of small wave heights and under prediction of large wave height events, when compared with measured waves in the La Grande Complex reservoirs. An in depth analysis was undertaken to eventually correct the formulas, with the objective being to accurately hindcast the wave hourly time series with locally measured wind data. The general form of the above equations is:

$$\frac{gH}{U_a^2} = \alpha_H \left(\frac{gF}{U_a^2}\right)^{\beta_H} \qquad \frac{gT}{U_a} = \alpha_T \left(\frac{gF}{U_a^2}\right)^{\beta_T} \quad [5]$$

with a power law assumed valid and therefore linear regression in the log-log domain of the dimensional variables yields the coefficient and exponent values for these equations. Duration is considered by establishing the celerity of the wave group in deep water, as follows:

$$\frac{C_g}{U_a} = \frac{1}{2}\left[\frac{\alpha_T}{2\pi}\left(\frac{gF}{U_a^2}\right)^{\beta_T}\right] \Rightarrow C_g = \frac{\alpha_T}{4\pi} g^{\beta_T} U_a^{1-2\beta_T} F^{1-\beta_T} \quad [6]$$

$$\int_0^t dt = \int_0^F \frac{dF}{C_g} = \frac{4\pi}{\alpha_T g^{\beta_T} U_a^{1-2\beta_T}} \int_0^F \frac{dF}{F^{\beta_T}} \quad [7]$$

$$\frac{gt}{U_a} = \frac{4\pi}{\alpha_T}\left(\frac{1}{1-\beta_T}\right)\left(\frac{gF}{U_a^2}\right)^{1-\beta_T} \quad [8]$$

Note that equation 8 is defined when $\alpha_T$ and $\beta_T$ are found.

Regression analysis is performed as an iterative process (figures 5a and 5b) which starts by first specifying starting values for $\alpha$ and $\beta$ in equation [5]. Equation [8] is then evaluated. Hourly time series are used and time duration is considered to evaluate the dimensional variables. Duration seldom extends beyond 3 hours due to the reservoir size and then only for mild wind states. Only peaks of events are retained when performing the regression. Results give a new set of coefficients and exponent values that affect the relation between duration and fetch length (equation 8). This iterative process converges to specific values of $\alpha$ and $\beta$. In parallel with this approach, multivariate analysis is performed to check the validity of the dimensional relations above. By expressing [5] in terms of *H*, one gets a relation in the form of [9] for which there is an additional constraint on exponent *c* which must equal:

2-2b.

Multivariate analysis performed on the data set gives exponent values for F and U that do not obey the above constraint (SEBJ, 1996b). In fact exponent "*c*" of *U* is found to be 1,21 for the dike TA-13 data set, which is quite close to the wind stress factor exponent (equation 10) given in SPM84. Based on this finding, all subsequent analyses are made with this wind stress factor:

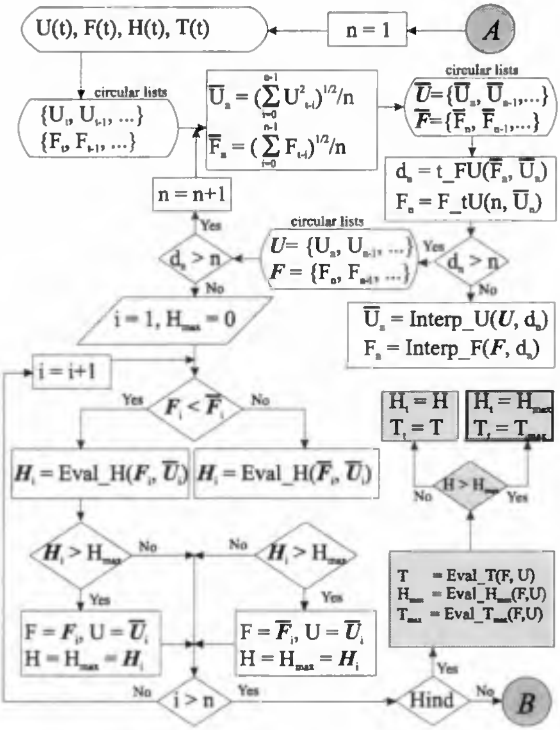


**Figure 5a.** Flowchart for dimensional analysis

$$H = \alpha_H g^{\beta_H - 1} F^{\beta_H} U^{2-2\beta_H} = aF^b U^c \qquad [9]$$

$$U_a = 0{,}71 \; U^{1{,}23} \qquad [10]$$

The fact that the wave steepness has a limiting value found to be in the vicinity of 0,06 for different fetch lengths and wind speed, implies that the exponent $\beta_H$ must be twice the value of the exponent $\beta_T$.

$$S=\frac{H}{L}=\frac{H}{\left(\frac{gT^2}{2\pi}\right)}=\frac{\left[\frac{gH}{U_a^2}\right]}{\frac{1}{2\pi}\left[\frac{gT}{U_a}\right]^2}=\frac{2\pi\alpha_H\left(\frac{gF}{U_a^2}\right)^{\beta_H}}{\alpha_T^2\left(\frac{gF}{U_a^2}\right)^{2\beta_T}}\Rightarrow\frac{2\pi\alpha_H}{\alpha_T^2}\quad if\quad \beta_H=2\beta_T \qquad [11]$$

This comes, from the definition for wave steepness(see equation 11) , that for $S$ to be constant, $F$ has to vanish, meaning $\beta_H = 2\beta_T$. The maximum wave steepness attainable is found to be theoretically equal to $2\pi\alpha_H / \alpha_T^2$.

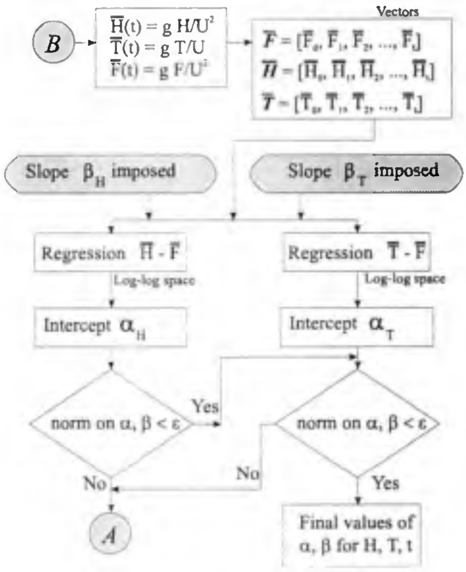


**Figure 5b.** Flowchart for dimensional analysis

## Dimensional analysis of site TA-13 data

Analysis is performed with a data set of over 9000 hourly values measured at the TA-13 mooring site. Figure 6 illustrates the body of water (in gray) along with the fetch evaluated following three different approaches (SPM77, SPM84 and the one proposed herein). Testing of different sector apertures were conducted (from 20 to 180 degrees), along with different weighting schemes ($\cos^2$, cos, unity). The use of a 180 degree sector with a $\cos^2$ weighting scheme, which is a Saville like fetch function, gave the best results for both regular and irregular shoreline cases. The fetch function is defined by the following equation:

$$F(\theta)=\frac{\sum_{\gamma=-90}^{90} R(\theta+\gamma)\ \cos^2(\gamma)}{\sum_{\gamma=-90}^{90}\cos(\gamma)} \qquad [12]$$

| | | | |
|---|---|---|---|
| with | $R(\theta)$ | Length of radial of heading $\theta$ | [m |
| | $F(\theta)$ | Length of fetch of heading $\theta$. | [m |
| | $\gamma$ | Angle formed by the radial and the central radial of the sector. | [°] |

A wave height of 0,5 m is chosen, as a lower threshold, in order to eliminate the influence of the buoy on the measurement of small waves. Analysis is first performed according to the procedures given in SPM77 and SPM84 (Table 1). The slope ($m_H$, $m_T$) and intercept values ($b_H$, $b_T$) of the scatter graph of predicted values against measured values are also listed (figure 7). For the SPM77, the wind speed $U$ is used. When the exponents are forced to the values proposed in the SPM, the difference in $\alpha_H$ are insignificant when compared to equations 3 and 4. This indicates that the wave climate of the reservoir is a short crested wave regime, no different then elsewhere, except for the mean period which is lower.

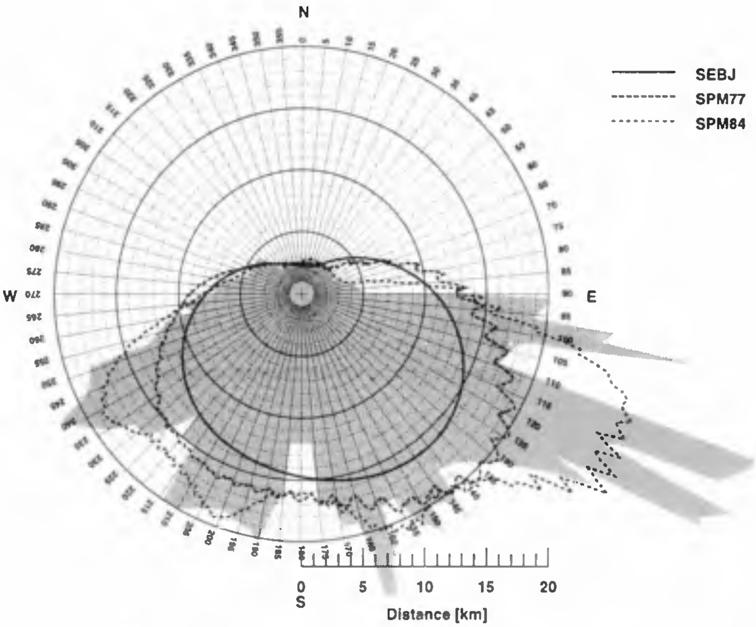


**Figure 6.** Fetch evaluation at mooring site TA-13

**Table 1.** Dimensional analysis results from dyke TA-13 data

| Method | $\beta_H$ | $\beta_T$ | $\alpha_H$ | $\alpha_T$ | $m_H$ | $b_H$ | $m_T$ | $b_T$ |
|---|---|---|---|---|---|---|---|---|
| SPM77 | 0,42[1] | 0,25[1] | 0,00363 | 0,462 | 0,73 | 0,24 | 0,78 | 0,7 |
| SPM84 | 0,50[1] | 0,33[1] | 0,00161 | 0,240 | 0,84 | 0,16 | 0,78 | 0,7 |
| SPM77 | 0,369 | 0,214 | 0,00521 | 0,602 | 0,79 | 0,19 | 0,90 | 0,3 |
| SPM84 | 0,374 | 0,187 | 0,00374 | 0,628 | 1,02 | -0,01 | 1,14 | -0,42 |
| SEBJ | 0,45[1] | 0,225[1] | 0,00247 | 0,509 | 0,87 | 0,12 | 0,99 | 0,04 |
| SEBJ | 0,467 | 0,238 | 0,00225 | 0,467 | 0,85 | 0,14 | 0,95 | 0,15 |

[1] Exponent value forced

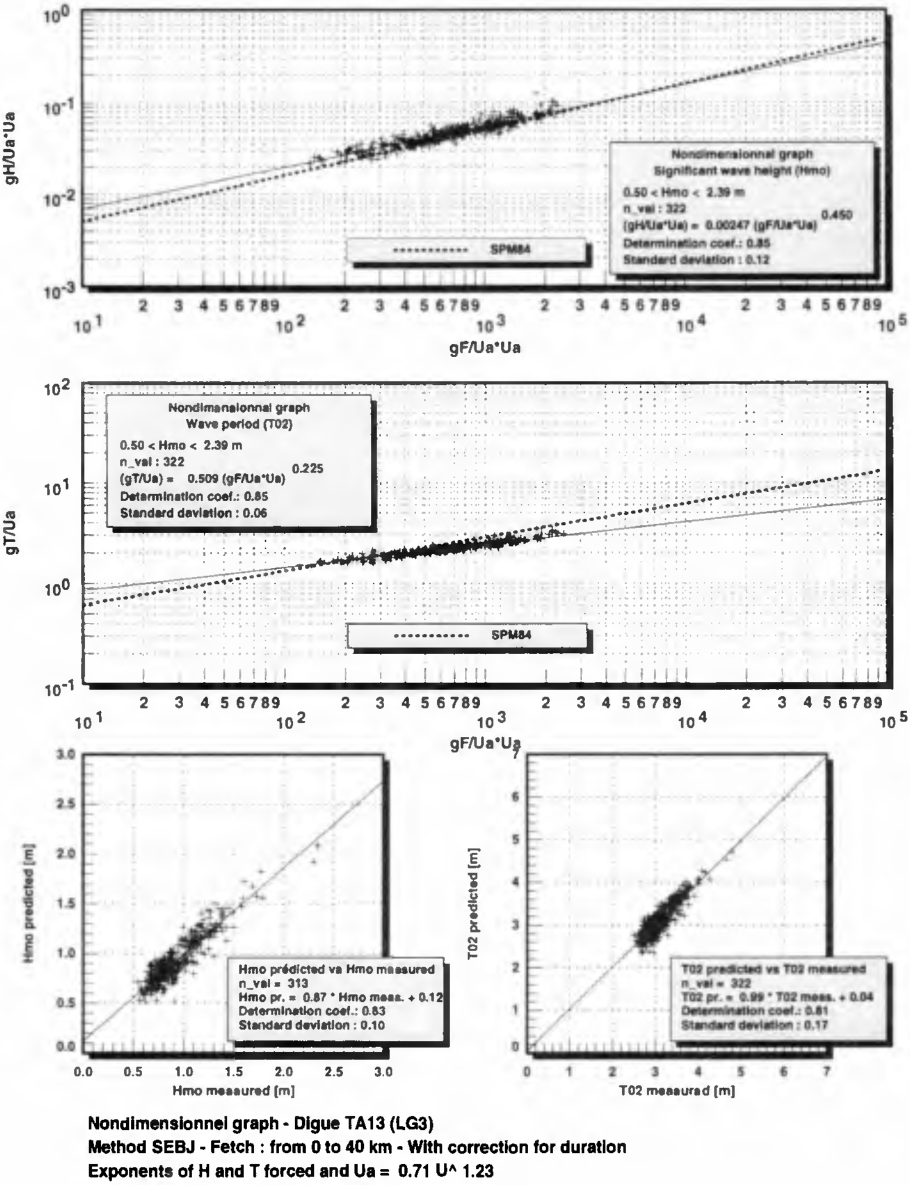


**Figure 7.** Example of dimensional analysis for mooring site TA-13

When exponents are let free to adjust, results are quite different, with lower values for the exponent and higher values for the coefficient. The maximum wave steepness, according to equation 11, are 0,084 and 0,074 respectively, which is high. The slopes from the scatter graphs indicate a tendency to under evaluate large wave episodes and over evaluate small wave episodes. Results from the analysis of dyke TA-13 yield exponent values of 0,467 and 0,238 respectively for which the ratio of exponent is near 1,96. The resulting wave steepness is found to be 0,065 which is a bit high but acceptable when compared with the values ranging from [0,06-0,065] obtained from measured data (figure 4). Since use of a common variable *($U_a$)* raised to a given power can have adverse effects on the quality of the regression (Kenney, 1993), the right set of parameters is chosen from a subset of results obtained by imposing the regression slope. Table 2 shows the results obtained, when the analysis is performed for different values of $\beta_H$ imposed with the constraint that $\beta_H$ is twice the value of $\beta_T$. In fact, by forcing the exponent to a given value, better prediction is obtained for $H_{mo}$ when $\beta_H$ is in the range [0,40-0,45] as it is shown on figure 8.

**Table 2.** Dimensional analysis results from dyke TA-13 data - $\beta$ forced

| $\beta_H$ | $\beta_T$ | $\alpha_H$ | $\alpha_T$ | $m_H$ | $b_H$ | $m_T$ | $b_T$ |
|---|---|---|---|---|---|---|---|
| 0,40 | 0,200 | 0,00341 | 0,598 | 0,94 | 0,06 | 1,05 | -0,17 |
| 0,43 | 0,215 | 0,00281 | 0,543 | 0,90 | 0,10 | 1,02 | -0,04 |
| 0,45 | 0,225 | 0,00247 | 0,509 | 0,87 | 0,12 | 0,99 | 0,04 |
| 0,47 | 0,235 | 0,00217 | 0,477 | 0,84 | 0,14 | 0,96 | 0,12 |
| 0,50 | 0,250 | 0,00179 | 0,433 | 0,80 | 0,18 | 0,92 | 0,17 |

SEBJ uses exponents of 0,45 and 0,225 which yield good prediction for waves in the range of the large measured wave episodes for both regular and irregular shorelines. The maximum wave steepness value is 0,06 which is the expected value.

## Hindcast procedure

Hindcast follows the same process used for dimensional analysis and shown in figure 5a, to evaluate wave height and period for a given hour. Figure 8 illustrates how hindcasted waves from overwater wind compare with measured waves at the buoy site. Both hindcasted and measured signals appear in the upper left. Shown in the upper right is the scatter graph and in the lower right is the ratio between computed and measured values as a function of direction. A perfect fit would mean that all values should lie on the unit circle. During the first year of measurements, influence of trees located in a particular sector of the island, at a greater distance than the recommended 10 times the height of the taller obstacle, was obvious, as the ratio went up. It is thus very important to locate wind stations far away from any obstacles, on flat land. Much of the scatter can be explained by time lag between signals due to the fast response of the water surface to quick change in wind state or to rapidly varying fetch length. This is one of the reason why a fetch defined by a large sector give a better results for a large variety of reservoir shoreline geometry. Notice that some short extreme wave episodes can be missed since the mean hourly wind speed is used and that the significant wave height value can change by more than 10% within an hour. Any event that lasts is fairly well reproduced. All hourly values are retained for regression in the scatter graph, which was not the case in dimensional analysis, where only peak values were considered. Hindcast at eight other sites gives similar results.

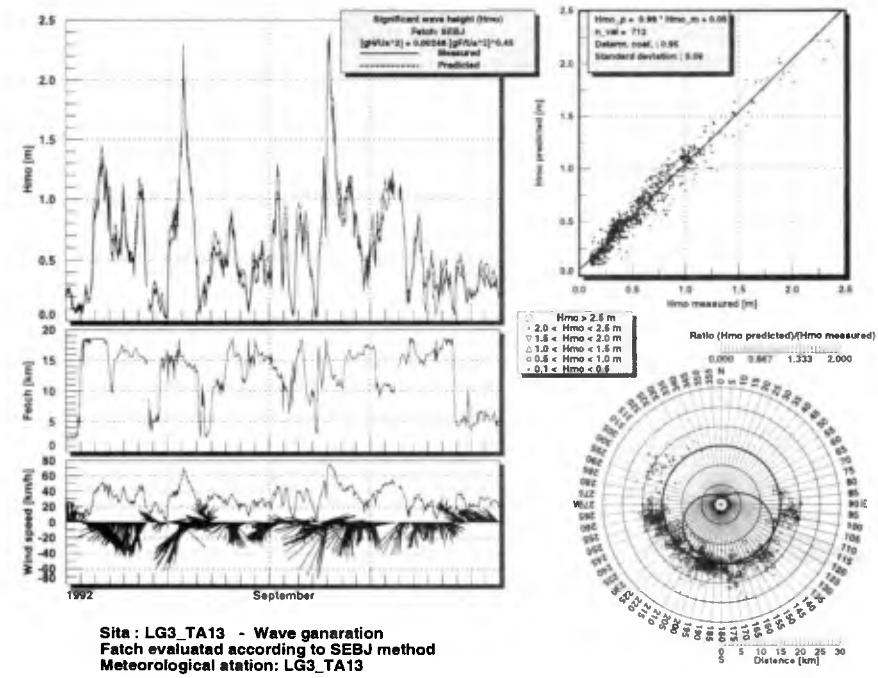


**Figure 8.** Example of wave hindcast from overwater wind data

## Wind overland and wind overwater

Hindcast for lengthy periods of time can be achieved only with airport meteorological stations. The weather stations (figure 9) were used to better define the transfer function between wind measured overland and wind measured overwater, three of which were located at nearby airports.

**Figure 9.** Retrieval of weather station in November

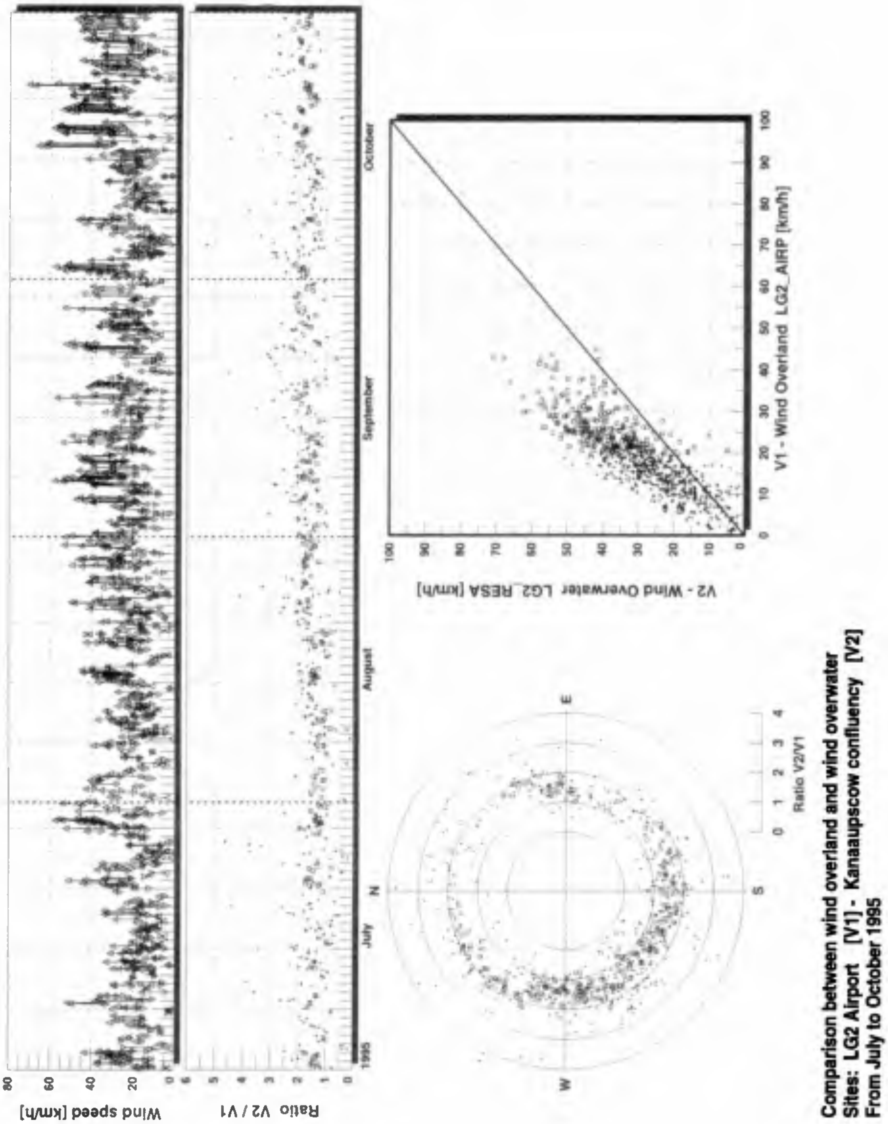


**Figure 10.** Wind overland and wind overwater

Records from both overland and overwater sites are visually inspected and punctual events are associated, to allow for the time lag between the two sites. All selected pairs are then plotted for further analysis. Figure 10 shows the results for one ice-free season. The scatter graph indicates that the wind overwater is larger but rarely exceeds the wind overland by more than 30 km/h. The way these points are distributed on the graph indicates that the ratio should decrease toward unity as the wind speed increases. Since there are only scarce measures for overland wind speed over 50 km/h, the relation can only be assumed for large values of wind speed. For design purposes and until sufficient data covering the upper region is obtained, the following relations are used to hindcast wave conditions from airport wind data:

$$U_w = 1{,}5 \;\; U_l \qquad \text{for } U_l \le 50 \text{ km/h}$$

$$U_w = 0{,}643 \;\; U_l + 42{,}9 \qquad \text{for } 50 < U_l < 120 \text{ km/h}$$

$$U_w = U_l \qquad \text{for } U_l \ge 120 \text{ km/h}$$

where $U_l$ and $U_w$ are respectively the wind overland and wind overwater in km/h.

## Hindcast with overland wind

Although this empirical relation needs more data for strong wind events, it has the advantage of being easy to implement and should yield a proper annual extreme event since most years will have events with extreme wind overland speed in the vicinity of 50 km/h. In this region, a ratio value of 1,5 yields the envelope curve of measured data. Quality of such procedure is checked using data from the La Grande Airport located 130 km west of site TA-13 for which waves were measured from 1992 to 1995. Results are shown in Table 3. Except for 1994, all differences are within 10%, which is satisfactory.

**Table 3.** Site TA-13. Measure and hindcast of annual extreme wave event.

| Year | Measure [m] | Hindcast [m] |
|---|---|---|
| 1992 | 2,39 | 2,25 |
| 1993 | 1,79 | 1,80 |
| 1994 | 1,17 | 1,34 |
| 1995 | 1,69 | 1,75 |

## Conclusion

Measurement of winds and waves in large reservoirs give good insight into wave generation by wind since the wave field is not contaminated by swell. The fast response of the reservoir is illustrated by the striking similarity between the wind speed and the significant wave height time series signals. Coefficients and exponents cannot be blindly evaluated from regression analysis in the log-log domain since use of a common variable raised to a given power can lead to false correlation. The fact that wave steepness, using $T_{02}$, has been measured to be a maximum value around 0,06 enables a relationship between $\alpha_H$ and $\beta_H$ to be derived and narrows the set of valid values from which to choose the correct pairs. The exponent of the dimensional wave height must be twice the value of the exponent for the mean wave period. For these conditions, it is possible to hindcast wave time series accurately with a model based on dimensional analysis, provided good quality overwater winds are used. Good quality wind hindcast for overland wind is then possible for long periods of time giving an effective tool for dam and dyke riprap design.

## Acknowledgements

The authors wish to thank La Société d'Énergie de la Baie James for permitting publication of this paper and Hydro-Québec for use of the information acquired during the mandate.

## References

Bretschneider C.L., 1964. *Generation of waves by wind. State of the art.* International Summer Course, Lunteren, The Netherlands, National Engineering Science Company, NESCO Report SN-134-6, Washington DC, September 1964, 96 p.

Caron O., P. Dupuis, T. Tran Van, 1993. *The Hydraulics of Riprap Design Applied to the Repairs of Dams and Dykes of the La Grande Hydroelectric Project.* Proceedings of the 5th Canadian Dam Safety Conference, St. John's, Nfld, September 1993.

CERC, 1977. *Shore Protection Manual.* U.S. Army Corps of Engineers, Coastal Engineering Research Center, Fort Belvoir, Virginia, 3 volumes, 1977 edition.

CERC, 1984. *Shore Protection Manual.* U.S. Army Corps of Engineers, Coastal Engineering Research Center, Fort Belvoir, Virginia, 3 volumes, 1984 edition.

IARH/PIANC, 1986. *List of Sea State Parameters.* PIANC Supplement to Bulletin no 52, Brussels, Belgium.

Kenney B.C., 1993. *On the validity of empirical power laws,* Stochastic Hydrology and Hydraulics, 7, pp. 179-194. Springer-Verlag.

Mansard E., M.H. Davies, O. Caron, 1996. *Model Study of Reservoir Riprap Stability.* 25th International Conference on Coastal Engineering, CERC-ASCE, Orlando, Florida, U.S.A, Book of abstracts, Paper no 94, September 1996.

SEBJ, 1996a *Mesures des vagues et du vent. Campagnes 1992-1995.* Rapport technique interne, Juin 1996, 56 p.

SEBJ, 1996b *Génération des vagues par le vent.* Rapport technique interne, Janvier 1996.

Tournier J.P., P. Dupuis, R. Arès, 1996. *An Improved Design Method for the Riprap of Earthfill Dams of Large Reservoirs.* 25th International Conference on Coastal Engineering, CERC-ASCE, Orlando, Florida, USA, Book of abstracts, Paper no 95, September 1996.